HHS Public Access

Author manuscript

Cell Signal. Author manuscript; available in PMC 2017 August 01.

Published in final edited form as:

Cell Signal. 2016 August ; 28(8): 798–809. doi:10.1016/j.cellsig.2016.03.013.

Negative regulation of the FOXO3a transcription factor by mTORC2 induces a pro-survival response following exposure to ultraviolet-B irradiation

Robert P. Feehan and **Lisa M. Shantz***

Department of Cellular and Molecular Physiology, Penn State University College of Medicine, Hershey, PA 17033

Abstract

Exposure to ultraviolet-B (UVB) irradiation, the principal cause of non-melanoma skin cancer (NMSC), activates both the rapamycin-sensitive mammalian target of rapamycin complex 1 (mTORC1) and the rapamycin-resistant mTORC2. We have previously reported that UVB-induced keratinocyte survival is dependent on mTORC2, though the specific mechanism is not well understood. FOXO3a is an important transcription factor involved in regulating cell survival. The activity of FOXO3a is reduced as a result of protein kinase B (AKT/PKB) activation, which is downstream of mTORC2; however, the specific function of FOXO3a during UVB-induced apoptosis is unclear. In this study, we establish that in cells with wild-type mTORC2 activity, FOXO3a is quickly phosphorylated in response to UVB and sequestered in the cytoplasm. In contrast, loss of mTORC2 causes FOXO3a to be localized to the nucleus and sensitizes cells to UVB-induced apoptosis. Furthermore, this sensitization is rescued by knockdown of FOXO3a. Taken together, these studies provide strong evidence that inhibition of mTORC2 enhances UVB-induced apoptosis in a FOXO3a-dependent manner, and suggest that FOXO3a activation by mTORC2 inhibitors may be a valuable chemopreventive target in NMSC.

Graphical Abstract

*Corresponding author: Lisa M. Shantz, Ph.D., The Penn State University College of Medicine, Department of Cellular and Molecular Physiology, Room C4731, 500 University Drive, Hershey, PA 17033. Tel: 717-531-1562; Fax: 717-531-7667, lms17@psu.edu (L. Shantz), rpf10@psu.edu (R. Feehan).

Conflict of Interest

The authors declare that they have no conflicts of interest with the content of this article.

Author Contributions

LMS and RPF designed the study and wrote the paper, as well as analyzed the results and approved the final version of the manuscript.

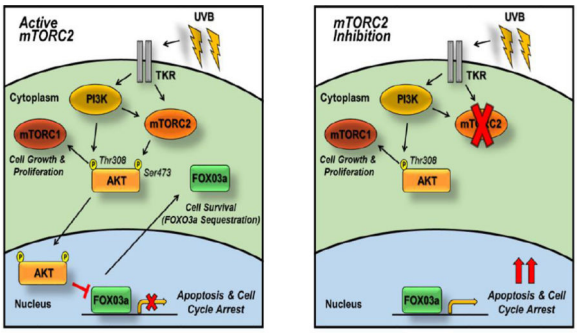

Increased Cell Survival Increased Apoptosis

Keywords

Keratinocyte; UVB; apoptosis; FOXO; mammalian target of rapamycin (mTOR); cancer chemoprevention

1. Introduction

The most significant environmental risk factor for developing non-melanoma skin cancer (NMSC) is ultraviolet-B irradiation (UVB) from both short and long term sun exposure [1]. Reported cases of NMSC have reached nearly 3.5 million in the United States alone, which is a remarkable 300% increase in diagnosed patients since 1994 [2]. Unlike other cancers where the incidence has stabilized or decreased, the rate of NMSC continues to rise, both within the general population and especially within high-risk groups, such as immunocompromised organ transplant recipients. The incidence of cutaneous squamous cell carcinoma (SCC) is 60–100-fold greater in organ transplant recipients than the general population, and frequently patients are diagnosed with multiple, aggressive SCCs [3, 4]. Thus, the identification of new therapeutic targets in NMSC has significant clinical implications. UVB exposure gives rise to mutations in critical genes as a result of DNA damage through generation of cyclobutane pyrimidine dimers and (6–4) photoproducts [5]. UVB also induces the activity of key signaling pathways involved in cellular maintenance and growth [6–10]. As a result, UVB is classified as a complete carcinogen, capable of both initiating and promoting tumorigenesis [11].

UVB irradiation activates the serine/threonine kinase mTOR (mammalian/mechanistic target of rapamycin) [8, 10, 12], which is at the center of an incompletely defined signaling network that responds to nutrients, growth factors, and cellular stress [13–15]. mTOR consists of two distinct signaling complexes: the rapamycin-sensitive mTOR complex 1 (mTORC1) and the rapamycin-resistant mTORC2 [14], which are both crucial in NMSC development following UVB exposure. Mutations in pathways that lead to mTOR signaling activation are frequently found in cancers, and this signaling network has been identified as a therapeutic target in several cancer types [13–15]. Activation of mTORC1 stimulates cell growth and proliferation in response to UVB [13, 14, 16–18]. Recent studies from our laboratory suggest that in addition to this mTORC1-dependent effect, mTORC2 signaling is also induced following UVB irradiation and promotes the survival of damaged cells [10, 12].

However, the mechanisms that regulate this survival process are not fully understood. Therefore, it is essential to characterize by what means mTOR controls cell survival upon UVB exposure. Understanding this phenomenon will aid in the development of targeted clinical therapies for patients with or at high risk for NMSC.

The studies described herein focus on the role of the transcription factor FOXO3a in the mTORC2-mediated survival response to UVB. FOXO3a is implicated as a key tumor suppressor and pro-apoptotic factor [19–27]. Regulation of FOXO3a is a multi-faceted process involving a large number of post-translational modifications including, but not limited to, phosphorylation by protein kinase B (AKT/PKB) [28–30], extracellular-signal-regulated kinase (ERK) [27, 31], mammalian sterile 20–like kinase-1 (MST1) [19], IκB kinase (IKK) [32, 33], and c-Jun N-terminal kinase 1 (JNK1) [34, 35], as well as deacetylation *via* silent mating type information regulation 2 homolog 1 (SIRT1) [36–38], and ubiquitination promoted by mouse double minute 2 homolog (MDM2) [39]. The primary emphasis of the work reported here is the AKT-specific phosphorylation of FOXO3a, which plays a negative regulatory role in the post-translational regulation of FOXO3a by reducing its activity through cytoplasmic sequestration [28, 40–45]. We have shown that AKT activation occurs in response to UVB exposure through induction of mTORC2 [10, 12]; however, a link between UVB irradiation and mTORC2-dependent FOXO3a regulation remains to be established. Thus, we hypothesize that UVB generates a unique anti-apoptotic response as a result of post-translational modifications of FOXO3a that are dependent on mTORC2.

2. Methods and Materials

2.1. Cell culture

HaCaT cells were obtained from the German Cancer Research Center and were used at passage <25 without further authentication. Mouse embryonic fibroblasts (MEFs) with inducible *rict* or knockout (iRictKO cells) or *raptor* knockout (iRapKO cells), a generous gift from Michael N. Hall (University of Basel - Biozentrum, Switzerland), were isolated from mice with either *rictor* or *raptor* conditional alleles, infected with a retrovirus carrying tamoxifen-inducible Cre recombinase ($CreER^{T2}$), and selected for stable integration of the virus as described previously [46]. Deletion of the floxed allele was induced by addition of 2 μM 4-hydroxytamoxifen (4OHT) to the cell culture medium for 72 h, which causes nuclear translocation of $CreER^{T2}$ and subsequent recombination. MEFs were used at passage <20 and were authenticated through PCR verification of the wild-type or floxed *rictor* or *raptor* allele. Absence of the recombined allele was verified through western blot analysis. All cell lines were monitored for consistent growth using growth curve analyses. The UVB and drug treatment experiments described below were started when cells had reached 70–80% confluence.

2.2. UVB and Drug Treatment

For UVB exposure, cells were washed twice with PBS, then in a minimal volume of PBS, the monolayer was exposed to UVB (FS20 UVB bulbs, National Biological, Cleveland OH) at doses indicated (20 or 35 mJ/cm^2). Bulb intensity was measured at the beginning of each

experiment using a UVB 500C meter (National Biological). After irradiation, PBS was removed and conditioned medium with drug treatments was added back. Torin 2 (Tocris Bioscience, Bristol UK), rapamycin (Developmental Therapeutics Program, National Cancer Institute), LY294002 (Tocris), the pan caspase inhibitor Z-VAD-FMK (Tocris), PD98059 (Tocris) or DMSO vehicle was added to the tissue culture medium at a 1:1000 dilution either overnight (Cell Viability, FACS, PD98059-treatment) or 1 h prior (Western & Immunofluorescence) to UVB treatment depending on the assay performed.

2.3. Western blotting analysis

Cells were washed twice with ice-cold PBS, harvested directly in 1× SDS sample buffer, and boiled for 5 min. Whole cell extracts were stored at −20°C until use. Western blotting was performed as described previously [10] using antibodies against Rictor, Raptor, mSIN1, AKT, p-AKT^{S473}, p-AKT^{T308}, S6K1, p-S6K1^{T389}, FOXO3a, p-FOXO1/3a$^{T24/T32}$, ERK1/2, P-ERK$^{T202/Y204}$, Caspase 3, PARP, α-Tubulin (1:1000 - Cell Signaling, Beverly MA), Lamin B1, (Cell Signaling, 1:500), and GAPDH (Cell Signaling, 1:2000). Comparisons of protein levels were normalized within the same gel and not between gels to allow for direct comparison of protein levels. Each blot is representative of at least two experiments with similar results as described in the figure legends. Note that due to the observed mTORC2-dependent, UVB-induced changes in total FOXO3a protein expression, P-FOXO3a^{T32} relative protein densities are normalized to the loading control and not total FOXO3a throughout this manuscript.

2.4. Lentiviral-mediated production and transduction

Lentiviral production was performed according to manufacturer's protocol (ViraPower™ Lentiviral Expression Systems, Life Technologies) using pLKO.1 constructs for sh-mSIN1 (mSin1 shRNA #1 from David Sabatini, Whitehead Institute for Biomedical Research, Cambridge MA, Addgene #13483), sh-Raptor (Raptor_1 shRNA from David Sabatini, Addgene #1857), sh-FOXO3a (Sigma-Aldrich, St. Louis MO - TRCN0000040102) and scrambled shRNA (scramble shRNA from David Sabatini, Addgene #1864). HaCaT cells were incubated with viral particles for 24–48 h and then selected with puromycin (1 μg/mL) in complete medium for 72 h following transduction. Double knockdown of FOXO3a and mSIN1 was accomplished through initial knockdown of FOXO3a as described above. The sh-FOXO3a cells were then subjected to a second transduction with sh-mSIN1 48 h prior to UVB exposure. Western blot analysis of mSIN1 and FOXO3a protein levels was performed to assess knockdown.

2.5. Immunofluorescence

Immunofluorescence was performed as described previously [47]. Briefly, cells were fixed with 3.7% paraformaldehyde and permeabilized with 0.2% Triton X-100 in 1× PBS. Cells were then blocked in 5% goat serum and incubated with anti-FOXO3a antibody (1:300 - Cell Signaling) overnight at 4°C. After primary antibody incubation and PBS wash, the cells were incubated with the Alexa Fluor 488 goat anti-rabbit secondary antibody (Molecular Probes | Life Technologies A-11008, 1:2500) for 1 h at room temperature and light protected. Cells were then counterstained with 300 nM DAPI and washed with 1× PBS prior to mounting with Fluoro-Gel (Electron Microscopy Sciences, Hatfield PA, 17983-20).

Images were viewed and captured with a Nikon microscope. Images shown are representative of 3 biological replicates with similar results.

2.6. Cellular Fractionation

Cellular fractionation of HaCaT and iRictKO cells was performed as described previously [48]. Briefly, the cells were pelleted, re-suspended in nuclear isolation buffer (10mM KCl, 10mM Tris, pH 7.5, 0.625% NP-40), incubated on ice for 20 min, and centrifuged at 1000×g at 4°C for 10 min. The supernatant was saved as the cytoplasmic fraction and further clarified by centrifugation at 16,000 × g for 10 min, which was then combined with 4× Laemmli Sample Buffer (4× LDS, Biorad). The nuclear pellet was washed three times with ice-cold 1× PBS, re-suspended in 4× LDS and run through a QIAshredder (Qiagen) at 16,000 × g for 2 min at room temperature. Both the cytoplasmic and nuclear samples were boiled for 5 min and then analyzed by Western blotting.

2.7. Cellular Transfection

HaCaT cells were grown to ~60% confluency and transfected with 2 μg of either an empty vector plasmid (pECE from William Rutter, University of California, San Francisco, Addgene plasmid #26453) or the HA-FOXO3a TM plasmid (from Michael Greenberg, Harvard Medical School, Cambridge, MA, Addgene plasmid # 1788) using Lipofectamine 2000 as per manufacturer's instructions (Invitrogen). UVB treatment was performed 48 h following transfection.

2.8. Cell Viability and Apoptosis Assays

Cell viability was determined colorimetrically by MTS assay (CellTiter 96 Aqueous Proliferation Assay, Promega) according to the manufacturer's instructions and monitored at 490 nm using a model 3550-UV plate reader (Biorad, Hercules CA). Each condition was plated using 12–18 biological replicates. Cell viability was calculated by setting the mean viability of the No-UVB control group to 100%. Apoptosis was assessed by flow cytometry using the Annexin V : PE Apoptosis Detection Kit I (BD Biosciences, Franklin Lakes NJ) according to the manufacturer's instructions. The percentage of early apoptotic (Annexin V positive / 7-Aminoactinomycin D [7-AAD] negative) and late apoptotic/necrotic (Annexin V / 7-AAD positive) cells was determined using a FACSCalibur cytometer (Beckman Coulter, Jersey City NJ) and analyzed with Modfit LT software (Verity Software). Fold change in apoptosis was calculated by taking the ratio of the percent of UVB-induced apoptotic cells over the percent of control No-UVB apoptotic cells within each experimental group. Cell viability and apoptosis experiments were repeated at least 3 times.

2.9. Statistics Analysis

Data directly comparing two groups (i.e. No-UVB vs UVB) were analyzed using the two-tailed Student's *t*-test. A two-way analysis of variance (ANOVA) was used when comparing interaction of the above values between groups (i.e. wild-type vs mTORC2-disrupted). Data were displayed as mean or percent change/fold difference ± standard deviation. Differences between values were considered significant when $p<0.05$. Experiments requiring t-test or

ANOVA analysis were repeated 2–3 times with at least 3 biological replicates per experimental group.

3. Results

3.1. Changes in FOXO3a phosphorylation and protein levels in response to UVB are dependent on mTOR signaling

Previous studies from our lab [10, 12] and others [8, 49] have demonstrated that UVB irradiation induces the pro-survival PI3-kinase (PI3K) and mTORC2 signaling pathways through downstream activation of AKT. AKT is activated by direct phosphorylation at Thr308 (P-AKT^{T308}) by phosphoinositide-dependent protein kinase-1 (PDK1), which is downstream of PI3K, and at Ser473 (P-AKT^{S473}) *via* mTORC2 [8–10, 12]. Other studies have shown that activated AKT can negatively regulate FOXO3a through direct phosphorylation [29, 40, 43]. With this in mind, we sought to determine the role of mTORC2 signaling in the regulation of FOXO3a phosphorylation in cells exposed to UVB. Based on previously published reports [9, 10, 12, 46, 50], we chose to use UVB-sensitive, spontaneously-immortalized, human keratinocytes (HaCaT cells) and 4OHT-inducible Rictor-deficient MEFs (iRictKO cells) for our model systems [12, 46]. In agreement with our previously described studies [10, 12], mTORC2 activity, as measured by phosphorylation of AKT at Ser473 (P-AKT^{S473}), was induced within 30 min and remained elevated for several hours following exposure to an apoptotic dose of UVB (20 mJ/cm^2) in both HaCaT (Fig. 1A - Scrambled) and iRictKO cells (Fig. 1B - DMSO). Likewise, FOXO3a was phosphorylated in this same time frame at the AKT target site Thr32 (P-FOXO3a^{T32}; Fig. 1A, B), which is an essential phosphorylation site responsible for the negative regulation of FOXO3a [29]. Interestingly, the induction of P-FOXO3a^{T32} in UVB-treated cells was accompanied by increased total FOXO3a protein levels in both HaCaT cells and MEFs with active mTORC2 activity (Fig. 1A, B).

Disruption of mTORC2 signaling was achieved through knockdown of either mSIN1 in HaCaT cells, or recombination of *rictor* in iRictKO cells, since both mSIN1 and Rictor are scaffolding proteins essential for proper mTORC2 function [51]. This disruption resulted in a reduction in UVB-induced P-AKT^{S473} while levels of the PDK1-specific P-AKT^{T308} were maintained (Fig. 1A - sh(mSIN1); Fig. 1B - 4OHT). This selective inhibition of P-AKT^{S473} by loss of either mSIN1 or Rictor confirms that mTORC2 signaling was impaired in our systems, while mTORC1-specific phosphorylation of AKT at Thr308 remained unaffected. Following UVB irradiation, both sh(mSIN1)-treated HaCaT cells and 4OHT-treated iRictKO cells exhibited sharp decreases in phosphorylated FOXO3a when compared to sh-scrambled HaCaT cells or DMSO-treated iRictKO cells respectively (Fig. 1A, B). In addition, total FOXO3a protein levels were greatly reduced over the 6 h time course (Fig. 1A, B). Taken together, these results suggest that both FOXO3a Thr32 phosphorylation and total protein expression are controlled in an mTORC2-dependent manner following exposure to UVB.

To verify that the UVB-induced reduction in FOXO3a phosphorylation and total protein were mediated by mTORC2, we disrupted the mTORC1 protein Raptor in HaCaT cells using shRNA directed toward Raptor (Fig. 2A), as well as employing inducible Raptor-deficient MEFs (iRapKO; Fig. 2B). In agreement with our previous results [10, 12], UVB

exposure activates mTORC1, as shown by phosphorylation of the ribosomal protein S6 kinase beta-1 (S6K1) at Thr389 (P-S6K1^{T389}; Fig. 2A, B). While the protein levels of Raptor appear to be moderately reduced following UVB in the DMSO-treated iRapKO cells, these cells also exhibit a robust induction of P-S6K1^{T389}, consistent with increased mTORC1 activity. Inhibition of mTORC1 in both the sh(Raptor)-treated HaCaT cells and iRapKO cells was verified by decreased phosphorylation of P-S6K1^{T389} (Fig. 2A, B). Unlike mTORC2 inhibition, loss of mTORC1 activity did not reduce P-AKT^{S473} in response to UVB (Fig. 2A, B). Similarly, there was no observed reduction in UVB-induced P-FOXO3a^{Thr32} or total FOXO3a protein when mTORC1 was inhibited (Fig. 2A, B). Interestingly, cells with disrupted mTORC1 signaling actually showed increases in both phosphorylated and total FOXO3a protein in response to UVB (Fig. 2A, B). The observed changes are most likely due to the reduction of an mTORC1-dependent negative feedback loop on mTORC2/PI3K activity [52, 53]. These results support the hypothesis that UVB-induced FOXO3a phosphorylation and protein expression are dependent on mTORC2 signaling.

To validate the genetic experiments above with pharmacological inhibitors, HaCaT cells were pre-treated with either the mTORC1-specific inhibitor rapamycin (Fig. S1A), the TOR-kinase inhibitor Torin 2 (Fig S1B), or DMSO prior to UVB irradiation. As expected, levels of P-AKT^{S473} were reduced in Torin 2- but not rapamycin-treated cells and the mTORC1-specific phosphorylation of S6K1 on Thr389 was reduced in the presence of either inhibitor (Fig. S1A, B). Immunoblot analysis shows that treatment with rapamycin did not reduce either phosphorylated or total FOXO3a protein expression when compared with the DMSO-treated group following UVB exposure (Fig. S1A). In contrast, pre-treatment with Torin 2, which inhibits both mTOR complexes, dramatically decreased both phosphorylated and total FOXO3a protein levels in UVB-treated cells (Fig. S1B). These results are consistent with the studies described above in which signaling through mTORC2 was disrupted. Moreover, rapamycin-treated HaCaT cells displayed increased UVB-induced FOXO3a protein expression (Fig. S1A), which is also consistent with both the sh(Raptor)-treated HaCaT cells and the 4OHT-treated iRapKO cells. Finally, cells treated with the PI3K inhibitor LY294002 (50 μM) responded identically to Torin 2-treated cells, confirming that the observed changes in FOXO3a are downstream of AKT activation (data not shown).

3.2. FOXO3a nuclear/cytoplasmic localization and abundance during the UVB time course is contingent on mTORC2 signaling

The mTORC2-dependent negative regulation of FOXO3a is reported to be a two-step process [28]. Initially, activated AKT enters the nucleus and phosphorylates FOXO3a, which allows the subsequent binding of the 14-3-3ζ chaperone protein dimer to nuclear FOXO3a. The interaction between 14-3-3ζ and FOXO3a reduces the binding of FOXO3a to DNA and facilitates the nuclear export and sequestration of the complex to the cytoplasm [29, 45, 54–56]. To examine the intracellular localization of FOXO3a in our system, both HaCaT and iRictKO cells were exposed to 20 mJ/cm^2 UVB and total FOXO3a was measured by immunofluorescence. Disruption of mTORC2 signaling in HaCaT cells was accomplished through shRNA knockdown of mSIN1, while mTOR signaling was chemically inhibited through pre-incubation with either Torin 2 (mTORC1/2 inhibitor) or rapamycin (mTORC1

inhibitor). Inhibition of mTORC2 in iRictKO cells was accomplished through 4OHT treatment. HaCaT cells with intact mTORC2 signaling showed a strong cytoplasmic localization of FOXO3a throughout the 3 h UVB time course (Fig. 3A - Scrambled; Fig. S2A). These results are as expected when considering previous studies on FOXO3a localization [28, 54] in conjunction with the induction of FOXO3a phosphorylation that we observed following UVB irradiation (Fig. 1A). Localization of the FOXO3a protein in the DMSO-treated iRictKO cells also remained primarily cytoplasmic following exposure to UVB (Fig. 3B, DMSO).

Inhibition of mTORC2 signaling in HaCaT cells caused a noticeable increase in nuclear FOXO3a localization (Fig. 3A - sh(mSIN1); Fig. S2B) compared to cells with active mTORC2. Disruption of mTORC2 in iRictKO cells (Fig. 3B - 4OHT) demonstrated similar localization of FOXO3a to the nucleus throughout the UVB time course when compared to DMSO-treated cells. It is also important to note that even prior to UVB irradiation, there was an apparent shift in the localization of FOXO3a from the cytoplasm to the nucleus following disruption of mTORC2 signaling (Fig. 3A, B; Fig. S2A, B – compare “No-UVB” time points). In contrast, rapamycin-treated HaCaT cells exhibited no apparent change in FOXO3a localization when compared to DMSO-treated cells at any point throughout the time course (Fig. S2C), suggesting that the observed localization response is dependent on mTORC2 inhibition.

The immunofluorescence images visibly demonstrate that disruption of mTORC2 increased relative nuclear FOXO3a localization when compared to cells with active mTORC2 signaling. However, these images do not distinguish whether this shift in localization is a result of increased nuclear FOXO3a protein abundance, or merely a decrease in cytoplasmic FOXO3a (i.e. *via* proteasomal degradation). As the immunoblot data from section 3.1 illustrates, total FOXO3a protein expression is reduced in mTORC2-disrupted cells following UVB exposure (Fig. 1). Therefore, it is possible the relative nuclear FOXO3a abundance may not actually change when mTORC2 is inhibited. To address this question, we performed nuclear/cytoplasmic fractionation of both HaCaT and iRictKO cells and measured FOXO3a protein expression in each compartment. Irrespective of mTORC2 activity levels, cytoplasmic FOXO3a followed an expression pattern similar to the whole cell immunoblot data (compare Fig. 1A, B to Fig. 3C, D - cytoplasm). Conversely, nuclear FOXO3a protein was noticeably increased following inhibition of mTORC2 signaling in both cell lines (Fig. 3C, D - nucleus), especially prior to UVB exposure (No-UVB). Taken together, even though total FOXO3a protein expression in whole cell extracts is decreased in cells with mTORC2 loss, both the relative nuclear localization and relative nuclear abundance of FOXO3a is increased in the absence of mTORC2.

3.3. Disruption of mTORC2 sensitizes HaCaT cells to apoptosis, which is rescued upon simultaneous knockdown of FOXO3a

Previous results from our lab showed an increased sensitivity to apoptosis in Rictor- and mTOR-ablated, chemically-induced tumors, as well as in Rictor$^{-/-}$ primary keratinocytes and MEFs upon UVB irradiation [10, 12]. In the present study, we demonstrated an mTORC2-dependent regulation of FOXO3a both before and after UVB exposure,

specifically in its phosphorylation, protein abundance, and relative localization. Therefore, we next examined whether UVB-induced apoptosis is directly related to the observed mTORC2-dependent FOXO3a regulation. To address this question, we inhibited the function of FOXO3a by shRNA knockdown in HaCaT cells, both in the presence or absence of mTORC2 inhibition via either mSIN1 knockdown (Fig. 4A) or Torin 2 treatment. We examined cell viability, as well as caspase 3 and PARP activation 24 h after exposure to UVB (35 mJ/cm^2). As expected, UVB reduced cell viability in vehicle-treated cells when compared to the No-UVB group, and disrupting mTORC2 signaling using either mSIN1 knockdown or Torin 2 treatment further reduced cell viability significantly (Fig. 4B, C). This reduction in cell viability in DMSO-treated cells was accompanied by increased caspase 3 and PARP activation (cleaved-caspase 3 and cleaved-PARP), which was further increased following treatment with Torin 2 (Fig. 4D, E). This is consistent with our previously reported data [10, 12]. Importantly, the increased UVB-induced cell death observed in both mTORC2-disrupted systems was rescued by simultaneous knockdown of FOXO3a (Fig. 4B–E).

It is important to note that knockdown of mSIN1 in HaCaT cells has an impact on cell viability measurements that is independent of UVB (Figure 4B – No UVB), which is in keeping with previous studies demonstrating that disruption of mTORC2 triggers accumulation of cells in G0/G1 and a reduction in S-phase cells [57]. Moreover, measuring changes in cell viability *via* MTS assay does not distinguish between increased apoptosis and changes in other cellular processes, but rather only measures viable cells. UVB exposure can both slow down cell cycle progression [58] and cause increased necrosis of HaCaT cells [59], both of which will decrease cell viability independent of apoptosis. Therefore, to assess caspase-dependent apoptosis, cell viability was measured in Torin 2-treated cells that were also treated with the pan-caspase inhibitor Z-VAD-FMK 12 h prior to UVB exposure. Exposure to Z-VAD-FMK was able to mimic the rescue in cell viability that was observed in Torin 2-treated cells with FOXO3a knockdown (Fig. 4C). Taken together, the above results suggest that mTORC2 inhibition stimulates FOXO3a specific, caspase-dependent apoptotic cell death in response to UVB.

To more precisely quantitate apoptosis in our systems, we used FACS staining for Annexin V & 7-AAD, which allows us to quantitatively distinguish between early apoptotic cells (Annexin V positive / 7-AAD negative) and late apoptotic/necrotic cells (Annexin V & 7-AAD positive). Unlike our cell viability measurements, there was no observed UVB-independent effect on apoptosis in the sh(mSIN1) HaCaT cells, as the percent of apoptotic cells following knockdown of mSIN1 was similar to control cells (Fig. S3B, 3G - Compare No-UVB groups). UVB irradiation (35 mJ/cm^2) produced a 3-fold increase in early apoptosis after 18 h in HaCaT cells when compared to their respective No-UVB samples analyzed at the same time point (Fig. 4F). Consistent with our previous studies [10], disrupting mTORC2 signaling either with knockdown of mSIN1 or Torin 2 treatment sensitized HaCaT cells to UVB-induced apoptosis, while there was no increase in apoptosis following mTORC1 inhibition with rapamycin, further suggesting a specific mTORC2-dependent effect (Fig 4F). Expressing a FOXO3a triple mutant that cannot be phosphorylated by AKT [29], which simulates the regulatory effects of mTORC2 inhibition on FOXO3a, resulted in a similar sensitization to apoptosis (Fig. 4F - FOXO3a (TM); Fig.

S3A). Most importantly, knockdown of FOXO3a in the mTORC2-disrupted HaCaT cells completely rescued the sensitization to UVB-induced apoptosis that was previously observed in these cells (Fig 4F). Total cell death (early apoptosis + late apoptosis/necrosis) followed a similar pattern (data not shown). Thus, these results demonstrate that inhibition of mTORC2 enhances UVB-induced apoptosis in a FOXO3a-dependent manner.

3.4. Dual inhibition of mTORC2 and MEK signaling increases nuclear localization of FOXO3a protein and further sensitizes HaCaT cells to UVB-induced apoptosis

In this study, we demonstrated that even though disruption of mTORC2 increases the FOXO3a-dependent apoptotic response to UVB, inhibition of mTORC2 considerably reduces total FOXO3a protein levels in UVB-treated cells. One potential mechanism responsible for this phenomenon may be the loss of mTORC2/AKT-dependent 14-3-3ζ binding to FOXO3a. Several studies suggest that in addition to cytoplasmic sequestration of FOXO3a, 14-3-3ζ provides a “protective barrier” for FOXO3a, which shields FOXO3a from dephosphorylation by protein phosphatase 2A (PP2A) and subsequent degradation induced by other post-translational modifications, one being through direct phosphorylation by the MEK/ERK pathway [28, 45]. We found that MEK activity (as measured by P-ERK$^{T202/Y204}$) was induced by UVB in both HaCaT and iRictKO cells independent of mTORC2 activity (Fig. S4A, B). Similar to AKT, studies show that when MEK phosphorylates and activates ERK, ERK can then phosphorylate FOXO3a in the nucleus and cause its exit into the cytoplasm. However, unlike mTORC2/AKT/14-3-3ζ regulation, the ERK-specific phosphorylation causes FOXO3a to be targeted for degradation *via* MDM2 [31]. This mechanism, along with our results, suggests that ERK could potentially regulate FOXO3a in the absence of mTORC2 signaling. Therefore, we decided to examine relative nuclear abundance of FOXO3a in mTORC2 disrupted cells after simultaneously inhibiting ERK using the MEK inhibitor PD98059.

MEK activity was inhibited in both HaCaT and iRictKO cells following overnight incubation with PD98059 (Fig. 5A, B; Fig S5). In agreement with the data presented in Figure 3, inhibition of mTORC2 in HaCaT cells (Fig. 5A - Torin 2) or iRictKO cells (Fig. 5B - 4OHT) increased nuclear FOXO3a abundance both before and following exposure to UVB. Interestingly, inhibition of MEK alone did not match the increase in nuclear FOXO3a observed as a result of mTORC2 inhibition, and only slightly increased FOXO3a nuclear abundance over vehicle-treated cells (Fig. 5A, B). However, inhibition of both mTORC2 and MEK signaling resulted in additional accumulation of nuclear FOXO3a protein compared to inhibition of either pathway alone, especially at shorter time points (Fig. 5A, B). These results suggest that dual inhibition of mTORC2 and MEK may further sensitize cells to FOXO3a-dependent, UVB-induced apoptosis when compared with mTORC2 disruption alone. To test this hypothesis, HaCaT cells treated with either DMSO, PD98059 (100μM), Torin 2 (50nM) or both PD98059 and Torin 2 were irradiated with 35 mJ/cm^2 UVB and apoptosis was analyzed by flow cytometry 18 h later. Inhibition of either MEK (PD98059) or mTORC2 (Torin 2) alone sensitized cells to apoptosis (Fig. 5C), and this sensitization was further increased following inhibition of both MEK and mTORC2 (Fig. 5C). Knocking down FOXO3a in cells treated with both inhibitors rescued the sensitization to UVB-

induced apoptosis (Fig 5C), further suggesting a FOXO3a-dependent effect. Analysis of total cell death resulted in a similar pattern (data not shown).

4. Discussion

In the present study, we demonstrate in several model systems that the mTORC2-dependent negative regulation of FOXO3a activates a survival response in UVB-treated cells. Using both genetic and pharmacological methods to alter mTOR and FOXO signaling, we determine that this effect requires the AKT-specific post-translational modification and cytoplasmic localization of FOXO3a, which can be reversed by disrupting mTORC2 signaling. These data provide strong evidence that induction of mTORC2 pathways in response to UVB promotes a downstream cell survival mechanism, which is mediated through reduction of the pro-apoptotic activity of FOXO3a.

Both mTOR complexes are critical in normal cell metabolism, development, and survival [14, 60, 61]. However, aberrant increases in mTOR signaling are found in a number of cancer types [13, 15, 62]. In the skin, reports show increased levels of both mTORC1 and mTORC2 activity during progression from normal keratinocytes to pre-cancerous actinic keratosis, and finally to NMSC [63]. Dysregulation of the mTOR pathway in keratinocytes is not limited to NMSC but has also been observed in multiple inflammatory skin diseases, including acne, psoriasis and dermatitis [64, 65]. In addition, it has been shown that mTORC1 inhibition with topical rapamycin blocks dermal inflammation that is associated with the hyperproliferative response to tumor promotion [66]. Using murine skin carcinogenesis models [10, 12], we demonstrated previously that mTORC1 is required for keratinocyte hyperproliferation in response to tumor promotion, whereas mTORC2 is necessary for tumor initiation through the survival of damaged keratinocytes. The current studies focus on FOXO3a, a known downstream target of mTORC2 and an important regulator of apoptosis in many diseases [22, 23, 26, 40, 44], including cancer [19, 20, 24, 27, 33]. Previous studies reveal that AKT, which is downstream of mTORC2, can phosphorylate and inhibit FOXO3a [28, 29, 40, 42, 45]. Here we investigated the relationship between mTORC2 signaling in response to UVB and subsequent regulation of FOXO3a.

While the FOX (Forkhead Box) superfamily of transcription factors is responsible for diverse cellular functions [24], the subclass of FOX”O” proteins primarily regulate cell cycle progression, oxidative stress, and cell survival functions [25, 26, 40]. FOXO3a is extensively post-translationally modified, with phosphorylation by AKT considered one of its primary negative regulators [40, 41, 62]. AKT is a critical regulator of many other cellular processes including metabolism, protein translation, and angiogenesis [67]. AKT plays a unique role in mTOR signaling, as its activation is both upstream of mTORC1 and downstream of mTORC2, and differential phosphorylation of residues Thr308 by PDK1 and Ser473 by mTORC2 alters the specificity of AKT for downstream targets [68]. Induction of the PI3K pathway results in Thr308-specific phosphorylation [60], which is sufficient to induce downstream mTORC1 signaling. However, studies suggest that AKT must be phosphorylated at both Thr308 and Ser473 in order to subsequently phosphorylate and regulate FOXO3a [67]. Using disruption of mTORC2 in HaCaT cells and MEFs through mSIN1 knockdown or *rictor* recombination, we specifically inhibit the Ser473

phosphorylation of AKT while maintaining phosphorylation of Thr308, which results in the downstream reduction of FOXO3a phosphorylation. Conversely, when we specifically inhibit mTORC1 activity, we see a rise in both UVB-induced P-AKT^{S473} and P-FOXO3a^{T32} levels. These results demonstrate that upon UVB irradiation, phosphorylation of AKT at Ser473 by mTORC2 is necessary for AKT-dependent FOXO3a regulation. The increase in P-AKT^{S473} and P-FOXO3a^{T32} seen with mTORC1 inhibition may stem from the reduction of an mTORC1-dependent, S6K1-specific negative feedback loop on mTORC2. S6K1 has been proposed to inhibit mTORC2 through direct phosphorylation of SIN1 [69]. Additionally, activation of S6K1 inhibits upstream PI3K signaling, which would indirectly decrease P-AKT^{T308} [53]. Recent studies suggest that there is a positive feedback loop between phosphorylation of AKT at Thr308 and mTORC2 activation, also mediated through SIN1 phosphorylation [52, 70]. Therefore, reducing S6K1 activity *via* mTORC1 inhibition could increase mTORC2 activity through either of these pathways in response to UVB. Upregulation of both mTOR and S6K1 has also been observed in the lesioned skin of a variety of inflammatory skin conditions [71, 72]. It would be interesting to determine whether mTORC1 inhibition has a similar effect on mTORC2 activity in these conditions.

The mTORC2-dependent negative regulation of FOXO3a results from 14-3-3ζ -directed cytoplasmic sequestration of FOXO3a [29, 40, 43]. Previous studies indicate that phosphorylation of FOXO3a by AKT at Thr32, Ser253, & Ser315 is not sufficient to reduce its activity. Rather, the 14-3-3ζ chaperone protein dimer recognizes this evolutionarily conserved motif, resulting in binding to FOXO3a at Thr32 and Ser253. This reduces the affinity of FOXO3a for DNA by masking the DNA binding domain [73]. In addition, 14-3-3ζ binding facilitates the cytoplasmic localization of FOXO3a by masking two nuclear localization sequences on the FOXO3a protein located near Ser253 [54]. This, along with two already exposed nuclear export signals on the carboxy terminus of FOXO3a, promotes the movement of FOXO3a out of the nucleus [28]. In this study, we use immunofluorescence imaging of FOXO3a to establish that FOXO3a remains predominantly cytoplasmic following UVB irradiation in cells with active mTORC2. Following disruption of mTORC2, we observe a strong nuclear localization of FOXO3a in cells prior to UVB exposure, which is maintained throughout the post-UVB time course. In addition, a concurrent increase in nuclear FOXO3a protein abundance is detected in mTORC2-disrupted cells using immunoblot analysis of nuclear and cytoplasmic cell extracts. Taken together, these results strongly suggest that cytoplasmic sequestration of FOXO3a is hindered in the absence of mTORC2 activity. It is also important to consider that the UVB-inducible kinases JNK1 and MST1 have been shown in other systems to positively regulate FOXO3a activity by facilitating nuclear entry [35, 74, 75]. Our results do not rule out the possibility that such a mechanism may also play a role in the observed FOXO3a nuclear localization in mTORC2-disrupted cells both before and after exposure to UVB.

In this present study, we demonstrate the novel finding that in addition to the cytoplasmic sequestration and UVB-induced phosphorylation of FOXO3a, cells with intact mTORC2 signaling also show a corresponding increase in total FOXO3a protein following UVB irradiation. Conversely, total FOXO3a protein levels in whole cell extracts, in conjunction with FOXO3a Thr32 phosphorylation, are reduced dramatically with disruption of mTORC2. Previous studies suggest that in addition to cytoplasmic sequestration, AKT-

dependent 14-3-3ζ binding also protects FOXO3a from dephosphorylation by PP2A, as well as degradation by other post-translational modifications [28, 45]. In addition, UVB-inducible kinases such as ERK [9] and IKK [76] decrease FOXO3a activity by promoting its nuclear export and MDM2-dependent degradation [27, 31, 33, 39, 77]. The combination of reduced AKT-dependent 14-3-3ζ binding and increased MDM2-dependent degradation may contribute to the dramatic decrease in total FOXO3a protein following UVB irradiation that we observe in mTORC2-disrupted cells. However, this UVB-induced whole cell decrease in FOXO3a protein is countered by both a sustained nuclear localization and an increased nuclear abundance of FOXO3a when compared to cells with active mTORC2. Therefore, these results suggest that even though mTORC2 inhibition reduces whole cell FOXO3a protein levels following UVB irradiation, overall the activity of FOXO3a is enhanced due to the relative increase in nuclear FOXO3a localization and abundance.

The studies described here validate and extend our previous results demonstrating an increased sensitivity to UVB-induced apoptosis upon inhibition of mTORC2 [10, 12]. UVB has been shown to promote both intrinsic and extrinsic apoptosis through increased activity of pro-apoptotic factors such as the *Trail* and *BIM*, which are both direct FOXO3a transcriptional targets [34, 49, 78] suggesting a FOXO3a-dependent effect. In agreement with this, the knockdown of FOXO3a in mTORC2 disrupted cells was able to rescue the UVB-induced sensitivity to apoptosis brought about by mTORC2 inhibition. These findings support the hypothesis that loss of mTORC2 signaling increases the pro-apoptotic activity of FOXO3a.

It is crucial to consider that environmental stressors such as UVB induce a complex stress response that may become pathologic [6]. Therefore, taking into consideration the multi-faceted regulation of FOXO3a is central to understanding how a stressor like UVB dictates FOXO3a expression and activity in keratinocytes. Several studies suggest that concurrent inhibition of other negative regulators of FOXO3a, along with the PI3K/mTORC2 pathway, may reduce drug resistance and enhance the activity of FOXO3a [22, 24, 30, 79, 80]. Specifically, reports show that inhibiting both the mTORC2/AKT and the MEK/ERK pathways, both of which are activated by UVB exposure, significantly increase the antitumor activity of FOXO3a in colon and pancreatic cancer models [27, 80, 81]. Here, we show that simultaneous inhibition of mTORC2 and MEK signaling increases relative FOXO3a nuclear abundance both before and immediately following UVB exposure, which coincides with an increased sensitization to UVB-induced apoptosis compared with either inhibitor alone. Furthermore, this process was shown to be FOXO3a-dependent as the effect was rescued following knockdown of FOXO3a. These results strongly point to combination therapy with a MEK inhibitor and TOR kinase inhibitor as a plausible option for NMSC prevention and treatment.

5. Conclusion

In summary, these studies demonstrate that UVB irradiation promotes the mTORC2-dependent cytoplasmic sequestration of FOXO3a, which is mediated by AKT. They further demonstrate the novel finding that this mTORC2-dependent negative regulation of FOXO3a is responsible for increased cell survival in response to UVB. Moreover, these studies reveal

that while inhibition of mTORC2 increases relative FOXO3a nuclear localization and abundance, it dramatically reduces whole cell FOXO3a protein levels in response to UVB, which may be due to proteasomal degradation *via* concurrent induction of an alternative UVB-inducible pathway such as MEK/ERK. In agreement with this idea, dual inhibition of mTORC2 and MEK signaling further increases both nuclear FOXO3a protein abundance and resulting UVB-induced apoptosis (see Fig. S7 for model). Future studies will be carried out to specifically explore the physiological stress response related to UVB-induced, FOXO3a-dependent apoptosis following combined mTORC2/MEK inhibition in keratinocytes.

Supplementary Material

Refer to Web version on PubMed Central for supplementary material.

Acknowledgments

We thank Nate Sheaffer, Jade Vogel and Joseph Bednarzyk from the Penn State Hershey Flow Cytometry Core Facility for help with flow cytometry analysis and Sherri Rennoll for critical reading of the manuscript. This work was supported by NIH grant ES019242 and the Pennsylvania Department of Health Tobacco CURE Funds to LMS. RPF is the recipient of an F31 predoctoral fellowship from NIH (ES026471).

Abbreviations

mTOR	mammalian target of rapamycin
UVB	ultraviolet-B
NMSC	non-melanoma skin cancer
mTORC1	mTOR complex 1
mTOC2	mTOR complex 2
AKT/PKB	protein kinase B
SCC	squamous cell carcinoma
ERK	extracellular-signal-regulated kinases
MEK	Mitogen-activated protein kinase/ERK kinase
PP2A	protein phosphatase 2A
MST1	mammalian sterile 20–like kinase-1
IKK	IκB kinase
JNK1	c-Jun N-terminal kinases 1
SIRT1	silent mating type information regulation 2 homolog 1
MDM2	mouse double minute 2 homolog
MEF	mouse embryonic fibroblasts

4OHT	4-hydroxytamoxifen
7-AAD	7-aminoactinomycin D
ANOVA	analysis of variance
PI3K	PI3-kinase
PDK1	phosphoinositide-dependent protein kinase-1
S6K1	ribosomal protein S6 kinase beta-1
FOX	forkhead box

References

1. Erb P, Ji J, Kump E, Mielgo A, Wernli M. Apoptosis and pathogenesis of melanoma and nonmelanoma skin cancer. Adv Exp Med Biol. 2008; 624:283–295. [PubMed: 18348464]
2. A.C. Society. , editor. ACS. Cancer facts and figures 2013. Atlanta: 2013.
3. Walsh SB, Xu J, Xu H, Kurundkar AR, Maheshwari A, Grizzle WE, Timares L, Huang CC, Kopelovich L, Elmets CA, Athar M. Cyclosporine a mediates pathogenesis of aggressive cutaneous squamous cell carcinoma by augmenting epithelial-mesenchymal transition: role of TGFbeta signaling pathway. Mol Carcinog. 2011; 50:516–527. [PubMed: 21308804]
4. Berg D, Otley CC. Skin cancer in organ transplant recipients: Epidemiology, pathogenesis, and management. J Am Acad Dermatol. 2002; 47:1–17. [PubMed: 12077575]
5. Patrick MH. Studies on thymine-derived UV photoproducts in DNA--I. Formation and biological role of pyrimidine adducts in DNA. Photochem Photobiol. 1977; 25:357–372. [PubMed: 882597]
6. Bowden GT. Prevention of non-melanoma skin cancer by targeting ultraviolet-B-light signalling. Nat Rev Cancer. 2004; 4:23–35. [PubMed: 14681688]
7. Cao C, Lu S, Jiang Q, Wang WJ, Song X, Kivlin R, Wallin B, Bagdasarian A, Tamakloe T, Chu WM, Marshall J, Kouttab N, Xu A, Wan Y. EGFR activation confers protections against UV-induced apoptosis in cultured mouse skin dendritic cells. Cell Signal. 2008; 20:1830–1838. [PubMed: 18644433]
8. Wan YS, Wang ZQ, Shao Y, Voorhees JJ, Fisher GJ. Ultraviolet irradiation activates PI 3-kinase/AKT survival pathway via EGF receptors in human skin in vivo. Int J Oncol. 2001; 18:461–466. [PubMed: 11179472]
9. Ming M, Han W, Maddox J, Soltani K, Shea CR, Freeman DM, He YY. UVB-induced ERK/AKT-dependent PTEN suppression promotes survival of epidermal keratinocytes. Oncogene. 2010; 29:492–502. [PubMed: 19881543]
10. Carr TD, DiGiovanni J, Lynch CJ, Shantz LM. Inhibition of mTOR suppresses UVB-induced keratinocyte proliferation and survival. Cancer Prev Res (Phila). 2012; 5:1394–1404. [PubMed: 23129577]
11. Ananthaswamy HN, Pierceall WE. Molecular mechanisms of ultraviolet radiation carcinogenesis. Photochem Photobiol. 1990; 52:1119–1136. [PubMed: 2087500]
12. Carr TD, Feehan RP, Hall MN, Rüegg MA, Shantz LM. Conditional disruption of rictor demonstrates a direct requirement for mTORC2 in skin tumor development and continued growth of established tumors. Carcinogenesis. 2015
13. Alayev A, Holz MK. mTOR signaling for biological control and cancer. J Cell Physiol. 2013; 228:1658–1664. [PubMed: 23460185]
14. Laplante M, Sabatini DM. mTOR signaling in growth control and disease. Cell. 2012; 149:274–293. [PubMed: 22500797]
15. Albanell J, Dalmases A, Rovira A, Rojo F. mTOR signalling in human cancer. Clin Transl Oncol. 2007; 9:484–493. [PubMed: 17720651]

16. Alessi DR, James SR, Downes CP, Holmes AB, Gaffney PR, Reese CB, Cohen P. Characterization of a 3-phosphoinositide-dependent protein kinase which phosphorylates and activates protein kinase Balpha. Curr Biol. 1997; 7:261–269. [PubMed: 9094314]
17. Brown EJ, Albers MW, Shin TB, Ichikawa K, Keith CT, Lane WS, Schreiber SL. A mammalian protein targeted by G1-arresting rapamycin-receptor complex. Nature. 1994; 369:756–758. [PubMed: 8008069]
18. Laplante M, Sabatini DM. Regulation of mTORC1 and its impact on gene expression at a glance. J Cell Sci. 2013; 126:1713–1719. [PubMed: 23641065]
19. Yu T, Ji J, Guo YL. MST1 activation by curcumin mediates JNK activation, Foxo3a nuclear translocation and apoptosis in melanoma cells. Biochem Biophys Res Commun. 2013; 441:53–58. [PubMed: 24134840]
20. Shukla S, Shukla M, Maclennan GT, Fu P, Gupta S. Deregulation of FOXO3A during prostate cancer progression. Int J Oncol. 2009; 34:1613–1620. [PubMed: 19424579]
21. Masui K, Tanaka K, Akhavan D, Babic I, Gini B, Matsutani T, Iwanami A, Liu F, Villa GR, Gu Y, Campos C, Zhu S, Yang H, Yong WH, Cloughesy TF, Mellinghoff IK, Cavenee WK, Shaw RJ, Mischel PS. mTOR complex 2 controls glycolytic metabolism in glioblastoma through FoxO acetylation and upregulation of c-Myc. Cell Metab. 2013; 18:726–739. [PubMed: 24140020]
22. Maiese K, Chong ZZ, Shang YC. OutFOXOing disease and disability: the therapeutic potential of targeting FoxO proteins. Trends Mol Med. 2008; 14:219–227. [PubMed: 18403263]
23. Maiese K, Chong ZZ, Shang YC. "Sly as a FOXO": new paths with Forkhead signaling in the brain. Curr Neurovasc Res. 2007; 4:295–302. [PubMed: 18045156]
24. Katoh M, Igarashi M, Fukuda H, Nakagama H, Katoh M. Cancer genetics and genomics of human FOX family genes. Cancer Lett. 2013; 328:198–206. [PubMed: 23022474]
25. Greer EL, Brunet A. FOXO transcription factors at the interface between longevity and tumor suppression. Oncogene. 2005; 24:7410–7425. [PubMed: 16288288]
26. Daitoku H, Fukamizu A. FOXO transcription factors in the regulatory networks of longevity. J Biochem. 2007; 141:769–774. [PubMed: 17569704]
27. Allen JE, Krigsfeld G, Mayes PA, Patel L, Dicker DT, Patel AS, Dolloff NG, Messaris E, Scata KA, Wang W, Zhou JY, Wu GS, El-Deiry WS. Dual inactivation of Akt and ERK by TIC10 signals Foxo3a nuclear translocation, TRAIL gene induction, and potent antitumor effects. Sci Transl Med. 2013; 5:171ra117.
28. Tzivion G, Dobson M, Ramakrishnan G. FoxO transcription factors; Regulation by AKT and 14-3-3 proteins. Biochim Biophys Acta. 2011; 1813:1938–1945. [PubMed: 21708191]
29. Brunet A, Bonni A, Zigmond MJ, Lin MZ, Juo P, Hu LS, Anderson MJ, Arden KC, Blenis J, Greenberg ME. Akt promotes cell survival by phosphorylating and inhibiting a Forkhead transcription factor. Cell. 1999; 96:857–868. [PubMed: 10102273]
30. Amente S, Zhang J, Lavadera ML, Lania L, Avvedimento EV, Majello B. Myc and PI3K/AKT signaling cooperatively repress FOXO3a-dependent PUMA and GADD45a gene expression. Nucleic Acids Res. 2011; 39:9498–9507. [PubMed: 21835778]
31. Yang JY, Zong CS, Xia W, Yamaguchi H, Ding Q, Xie X, Lang JY, Lai CC, Chang CJ, Huang WC, Huang H, Kuo HP, Lee DF, Li LY, Lien HC, Cheng X, Chang KJ, Hsiao CD, Tsai FJ, Tsai CH, Sahin AA, Muller WJ, Mills GB, Yu D, Hortobagyi GN, Hung MC. ERK promotes tumorigenesis by inhibiting FOXO3a via MDM2-mediated degradation. Nat Cell Biol. 2008; 10:138–148. [PubMed: 18204439]
32. Xu Y, Lai E, Liu J, Lin J, Yang C, Jia C, Li Y, Bai X, Li M. IKK interacts with rictor and regulates mTORC2. Cell Signal. 2013; 25:2239–2245. [PubMed: 23872070]
33. Hu MC, Lee DF, Xia W, Golfman LS, Ou-Yang F, Yang JY, Zou Y, Bao S, Hanada N, Saso H, Kobayashi R, Hung MC. IkappaB kinase promotes tumorigenesis through inhibition of forkhead FOXO3a. Cell. 2004; 117:225–237. [PubMed: 15084260]
34. Bivik C, Ollinger K. JNK mediates UVB-induced apoptosis upstream lysosomal membrane permeabilization and Bcl-2 family proteins. Apoptosis. 2008; 13:1111–1120. [PubMed: 18651223]
35. Chaanine AH, Jeong D, Liang L, Chemaly ER, Fish K, Gordon RE, Hajjar RJ. JNK modulates FOXO3a for the expression of the mitochondrial death and mitophagy marker BNIP3 in pathological hypertrophy and in heart failure. Cell Death Dis. 2012; 3:265. [PubMed: 22297293]

36. Brunet A, Sweeney LB, Sturgill JF, Chua KF, Greer PL, Lin Y, Tran H, Ross SE, Mostoslavsky R, Cohen HY, Hu LS, Cheng HL, Jedrychowski MP, Gygi SP, Sinclair DA, Alt FW, Greenberg ME. Stress-dependent regulation of FOXO transcription factors by the SIRT1 deacetylase. Science. 2004; 303:2011–2015. [PubMed: 14976264]
37. Giannakou ME, Partridge L. The interaction between FOXO and SIRT1: tipping the balance towards survival. Trends Cell Biol. 2004; 14:408–412. [PubMed: 15308206]
38. Daitoku H, Sakamaki J, Fukamizu A. Regulation of FoxO transcription factors by acetylation and protein-protein interactions. Biochim Biophys Acta. 2011; 1813:1954–1960. [PubMed: 21396404]
39. Fu W, Ma Q, Chen L, Li P, Zhang M, Ramamoorthy S, Nawaz Z, Shimojima T, Wang H, Yang Y, Shen Z, Zhang Y, Zhang X, Nicosia SV, Zhang Y, Pledger JW, Chen J, Bai W. MDM2 acts downstream of p53 as an E3 ligase to promote FOXO ubiquitination and degradation. J Biol Chem. 2009; 284:13987–14000. [PubMed: 19321440]
40. Zhang X, Tang N, Hadden TJ, Rishi AK. Akt, FoxO and regulation of apoptosis. Biochim Biophys Acta. 2011; 1813:1978–1986. [PubMed: 21440011]
41. Xie Q, Chen J, Yuan Z. Post-translational regulation of FOXO. Acta Biochim Biophys Sin (Shanghai). 2012; 44:897–901. [PubMed: 22935512]
42. Singh A, Ye M, Bucur O, Zhu S, Tanya Santos M, Rabinovitz I, Wei W, Gao D, Hahn WC, Khosravi-Far R. Protein phosphatase 2A reactivates FOXO3a through a dynamic interplay with 14-3-3 and AKT. Mol Biol Cell. 2010; 21:1140–1152. [PubMed: 20110348]
43. Kloet DE, Burgering BM. The PKB/FOXO switch in aging and cancer. Biochim Biophys Acta. 2011; 1813:1926–1937. [PubMed: 21539865]
44. Hay N. Interplay between FOXO, TOR, and Akt. Biochim Biophys Acta. 2011; 1813:1965–1970. [PubMed: 21440577]
45. Dobson M, Ramakrishnan G, Ma S, Kaplun L, Balan V, Fridman R, Tzivion G. Bimodal regulation of FoxO3 by AKT and 14-3-3. Biochim Biophys Acta. 2011; 1813:1453–1464. [PubMed: 21621563]
46. Cybulski N, Zinzalla V, Hall MN. Inducible raptor and rictor knockout mouse embryonic fibroblasts. Methods Mol Biol. 2012; 821:267–278. [PubMed: 22125071]
47. Konsavage WM Jr, Kyler SL, Rennoll SA, Jin G, Yochum GS. Wnt/beta-catenin signaling regulates Yes-associated protein (YAP) gene expression in colorectal carcinoma cells. J Biol Chem. 2012; 287:11730–11739. [PubMed: 22337891]
48. Yochum GS, Cleland R, McWeeney S, Goodman RH. An antisense transcript induced by Wnt/beta-catenin signaling decreases E2F4. J Biol Chem. 2007; 282:871–878. [PubMed: 17121828]
49. Kim DJ, Kataoka K, Sano S, Connolly K, Kiguchi K, DiGiovanni J. Targeted disruption of Bcl-xL in mouse keratinocytes inhibits both UVB- and chemically induced skin carcinogenesis. Mol Carcinog. 2009; 48:873–885. [PubMed: 19309000]
50. Boukamp P, Petrussevska RT, Breitkreutz D, Hornung J, Markham A, Fusenig NE. Normal keratinization in a spontaneously immortalized aneuploid human keratinocyte cell line. J Cell Biol. 1988; 106:761–771. [PubMed: 2450098]
51. Frias MA, Thoreen CC, Jaffe JD, Schroder W, Sculley T, Carr SA, Sabatini DM. mSin1 is necessary for Akt/PKB phosphorylation, and its isoforms define three distinct mTORC2s. Curr Biol. 2006; 16:1865–1870. [PubMed: 16919458]
52. Yang G, Murashige DS, Humphrey SJ, James DE. A Positive Feedback Loop between Akt and mTORC2 via SIN1 Phosphorylation. Cell Rep. 2015; 12:937–943. [PubMed: 26235620]
53. O'Reilly KE, Rojo F, She QB, Solit D, Mills GB, Smith D, Lane H, Hofmann F, Hicklin DJ, Ludwig DL, Baselga J, Rosen N. mTOR inhibition induces upstream receptor tyrosine kinase signaling and activates Akt. Cancer Res. 2006; 66:1500–1508. [PubMed: 16452206]
54. Brunet A, Kanai F, Stehn J, Xu J, Sarbassova D, Frangioni JV, Dalal SN, DeCaprio JA, Greenberg ME, Yaffe MB. 14-3-3 transits to the nucleus and participates in dynamic nucleocytoplasmic transport. J Cell Biol. 2002; 156:817–828. [PubMed: 11864996]
55. Cahill CM, Tzivion G, Nasrin N, Ogg S, Dore J, Ruvkun G, Alexander-Bridges M. Phosphatidylinositol 3-kinase signaling inhibits DAF-16 DNA binding and function via 14-3-3-dependent and 14-3-3-independent pathways. J Biol Chem. 2001; 276:13402–13410. [PubMed: 11124266]

56. Silhan J, Vacha P, Strnadova P, Vecer J, Herman P, Sulc M, Teisinger J, Obsilova V, Obsil T. 14-3-3 protein masks the DNA binding interface of forkhead transcription factor FOXO4. J Biol Chem. 2009; 284:19349–19360. [PubMed: 19416966]
57. Rosner M, Fuchs C, Siegel N, Valli A, Hengstschlager M. Functional interaction of mammalian target of rapamycin complexes in regulating mammalian cell size and cell cycle. Hum Mol Genet. 2009; 18:3298–3310. [PubMed: 19505958]
58. Gentile M, Latonen L, Laiho M. Cell cycle arrest and apoptosis provoked by UV radiation-induced DNA damage are transcriptionally highly divergent responses. Nucleic Acids Res. 2003; 31:4779–4790. [PubMed: 12907719]
59. Mammone T, Gan D, Collins D, Lockshin RA, Marenus K, Maes D. Successful separation of apoptosis and necrosis pathways in HaCaT keratinocyte cells induced by UVB irradiation. Cell Biol Toxicol. 2000; 16:293–302. [PubMed: 11201053]
60. Hemmings BA, Restuccia DF. PI3K-PKB/Akt pathway. Cold Spring Harb Perspect Biol. 2012; 4:a011189. [PubMed: 22952397]
61. Shimobayashi M, Hall MN. Making new contacts: the mTOR network in metabolism and signalling crosstalk. Nat Rev Mol Cell Biol. 2014; 15:155–162. [PubMed: 24556838]
62. Engelman JA. Targeting PI3K signalling in cancer: opportunities, challenges and limitations. Nat Rev Cancer. 2009; 9:550–562. [PubMed: 19629070]
63. Einspahr JG, Calvert V, Alberts DS, Curiel-Lewandrowski C, Warneke J, Krouse R, Stratton SP, Liotta L, Longo C, Pellacani G, Prasad A, Sagerman P, Bermudez Y, Deng J, Bowden GT, Petricoin EF 3rd. Functional protein pathway activation mapping of the progression of normal skin to squamous cell carcinoma. Cancer Prev Res (Phila). 2012; 5:403–413. [PubMed: 22389437]
64. Balato A, Caprio RD, Lembo S, Mattii M, Megna M, Schiattarella M, Tarantino G, Balato N, Ayala F, Monfrecola G. Mammalian Target of Rapamycin in Inflammatory Skin Conditions. European Journal of Inflamation. 2014; 12:341–350.
65. Monfrecola G, Balato A, Caiazzo G, De Vita V, Di Caprio R, Donnarumma M, Lembo S, Fabbrocini G. Mammalian target of rapamycin, insulin resistance and hidradenitis suppurativa: a possible metabolic loop. J Eur Acad Dermatol Venereol. 2015
66. Checkley LA, Rho O, Moore T, Hursting S, DiGiovanni J. Rapamycin is a potent inhibitor of skin tumor promotion by 12-O-tetradecanoylphorbol-13-acetate. Cancer Prev Res (Phila). 2011; 4:1011–1020. [PubMed: 21733825]
67. Manning BD, Cantley LC. AKT/PKB signaling: navigating downstream. Cell. 2007; 129:1261–1274. [PubMed: 17604717]
68. Jacinto E, Facchinetti V, Liu D, Soto N, Wei S, Jung SY, Huang Q, Qin J, Su B. SIN1/MIP1 maintains rictor-mTOR complex integrity and regulates Akt phosphorylation and substrate specificity. Cell. 2006; 127:125–137. [PubMed: 16962653]
69. Liu P, Gan W, Inuzuka H, Lazorchak AS, Gao D, Arojo O, Liu D, Wan L, Zhai B, Yu Y, Yuan M, Kim BM, Shaik S, Menon S, Gygi SP, Lee TH, Asara JM, Manning BD, Blenis J, Su B, Wei W. Sin1 phosphorylation impairs mTORC2 complex integrity and inhibits downstream Akt signalling to suppress tumorigenesis. Nat Cell Biol. 2013; 15:1340–1350. [PubMed: 24161930]
70. Humphrey SJ, Yang G, Yang P, Fazakerley DJ, Stockli J, Yang JY, James DE. Dynamic adipocyte phosphoproteome reveals that Akt directly regulates mTORC2. Cell Metab. 2013; 17:1009–1020. [PubMed: 23684622]
71. Buerger C, Malisiewicz B, Eiser A, Hardt K, Boehncke WH. Mammalian target of rapamycin and its downstream signalling components are activated in psoriatic skin. Br J Dermatol. 2013; 169:156–159. [PubMed: 23398394]
72. Monfrecola G, Lembo S, Caiazzo G, De Vita V, Di Caprio R, Balato A, Fabbrocini G. Mechanistic target of rapamycin (mTOR) expression is increased in acne patients' skin. Exp Dermatol. 2016; 25:153–155. [PubMed: 26477999]
73. Obsil T, Ghirlando R, Anderson DE, Hickman AB, Dyda F. Two 14-3-3 binding motifs are required for stable association of Forkhead transcription factor FOXO4 with 14-3-3 proteins and inhibition of DNA binding. Biochemistry. 2003; 42:15264–15272. [PubMed: 14690436]

74. Lu C, Shi Y, Luo Y, Duan L, Hou Y, Hu H, Wang Z, Xiang P. MAPKs and Mst1/Caspase-3 pathways contribute to H2B phosphorylation during UVB-induced apoptosis. Sci China Life Sci. 2010; 53:663–668. [PubMed: 20602268]

75. Ardestani A, Paroni F, Azizi Z, Kaur S, Khobragade V, Yuan T, Frogne T, Tao W, Oberholzer J, Pattou F, Kerr Conte J, Maedler K. MST1 is a key regulator of beta cell apoptosis and dysfunction in diabetes. Nat Med. 2014; 20:385–397. [PubMed: 24633305]

76. Witt J, Barisic S, Schumann E, Allgower F, Sawodny O, Sauter T, Kulms D. Mechanism of PP2A-mediated IKK beta dephosphorylation: a systems biological approach. BMC Syst Biol. 2009; 3:71. [PubMed: 19607706]

77. Huang H, Tindall DJ. Regulation of FOXO protein stability via ubiquitination and proteasome degradation. Biochim Biophys Acta. 2011; 1813:1961–1964. [PubMed: 21238503]

78. Qin JZ, Bacon P, Panella J, Sitailo LA, Denning MF, Nickoloff BJ. Low-dose UV-radiation sensitizes keratinocytes to TRAIL-induced apoptosis. J Cell Physiol. 2004; 200:155–166. [PubMed: 15137068]

79. Tenbaum SP, Ordonez-Moran P, Puig I, Chicote I, Arques O, Landolfi S, Fernandez Y, Herance JR, Gispert JD, Mendizabal L, Aguilar S, Ramon y Cajal S, Schwartz S Jr, Vivancos A, Espin E, Rojas S, Baselga J, Tabernero J, Munoz A, Palmer HG. beta-catenin confers resistance to PI3K and AKT inhibitors and subverts FOXO3a to promote metastasis in colon cancer. Nat Med. 2012; 18:892–901. [PubMed: 22610277]

80. Roy SK, Srivastava RK, Shankar S. Inhibition of PI3K/AKT and MAPK/ERK pathways causes activation of FOXO transcription factor, leading to cell cycle arrest and apoptosis in pancreatic cancer. J Mol Signal. 2010; 5:10. [PubMed: 20642839]

81. Prabhu VV, Allen JE, Dicker DT, El-Deiry WS. Small-Molecule ONC201/TIC10 Targets Chemotherapy-Resistant Colorectal Cancer Stem-like Cells in an Akt/Foxo3a/TRAIL-Dependent Manner. Cancer Res. 2015; 75:1423–1432. [PubMed: 25712124]

Highlights

- Regulation of FOXO3a protein is dependent on mTOR signaling in response to UVB.
- Inhibition of mTORC2 signaling increases nuclear localization of FOXO3a
- Disruption of mTORC2 sensitizes cells to FOXO3a-dependent, UVB-induced apoptosis.
- FOXO3a activation by mTORC2 inhibitors may assist in skin cancer chemoprevention.

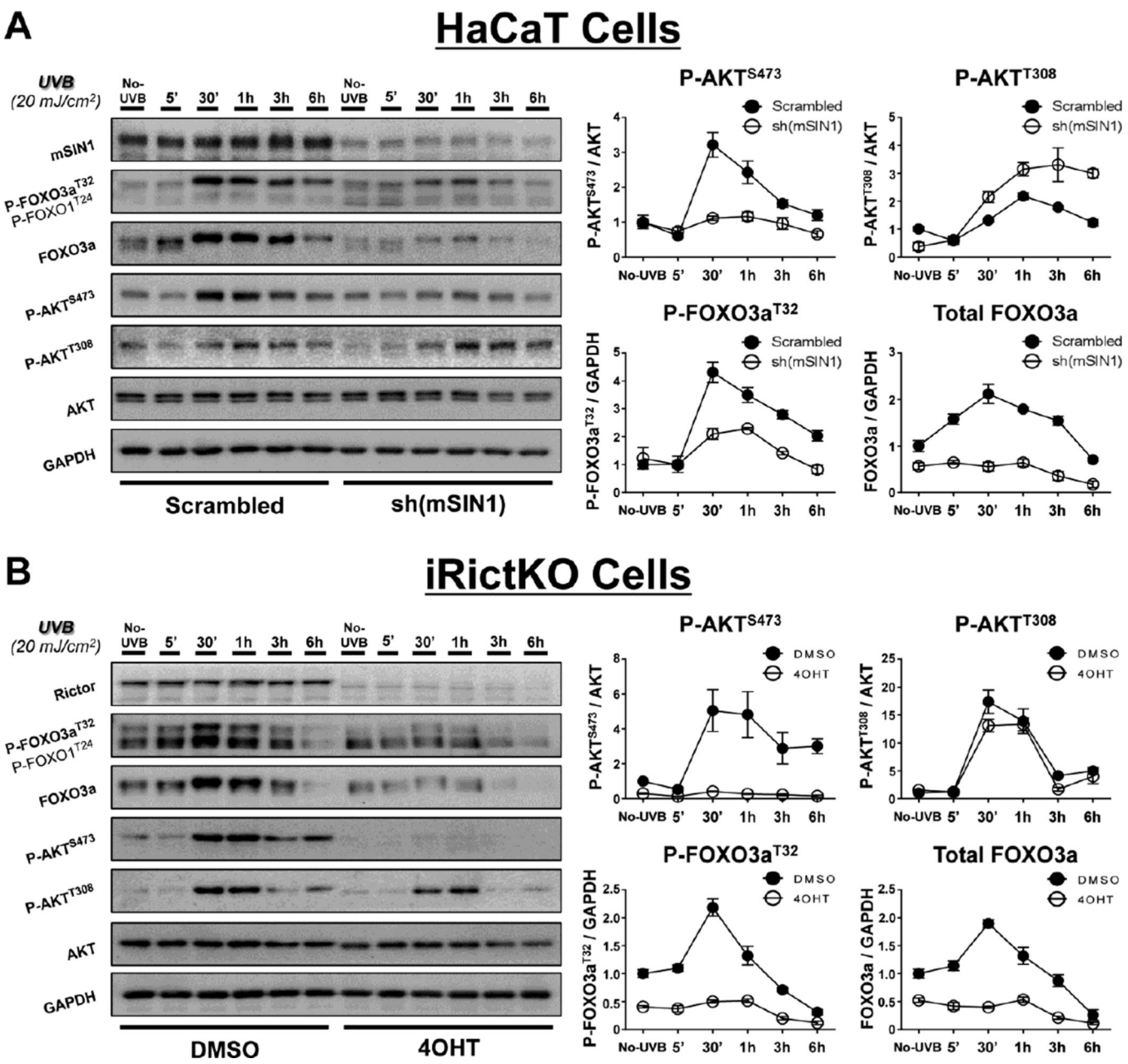

Fig. 1. Genetic disruption of mTORC2 inhibits FOXO3a phosphorylation and reduces FOXO3a protein levels in response to UVB

Immunoblot analysis (whole-cell extracts) of mTORC2 signaling during a 6 h UVB (20mJ/cm^2) time course in **(A)** HaCaT or **(B)** iRictKO cells with intact or disrupted mTORC2 activity. Cells were harvested at the indicated times post-UVB and western blotting was performed with antibodies directed to mTOR signaling intermediates. Disruption of mTORC2 was achieved as described in the Materials and Methods through **(A)** shRNA knockdown of mSIN1 in HaCaT cells [sh(mSIN1)] or **(B)** 4OHT-induced recombination of a floxed *rictor* allele in iRictKO cells (4OHT), and compared to their respective controls (Scrambled or DMSO). The relative protein densities for both P-AKT^{S473} and P-AKT^{T308} were normalized to their respective total protein while both P-

FOXO3a^{T32} and total FOXO3a were normalized to GAPDH. Quantitation of results is presented as the mean ± SEM of three independent experiments.

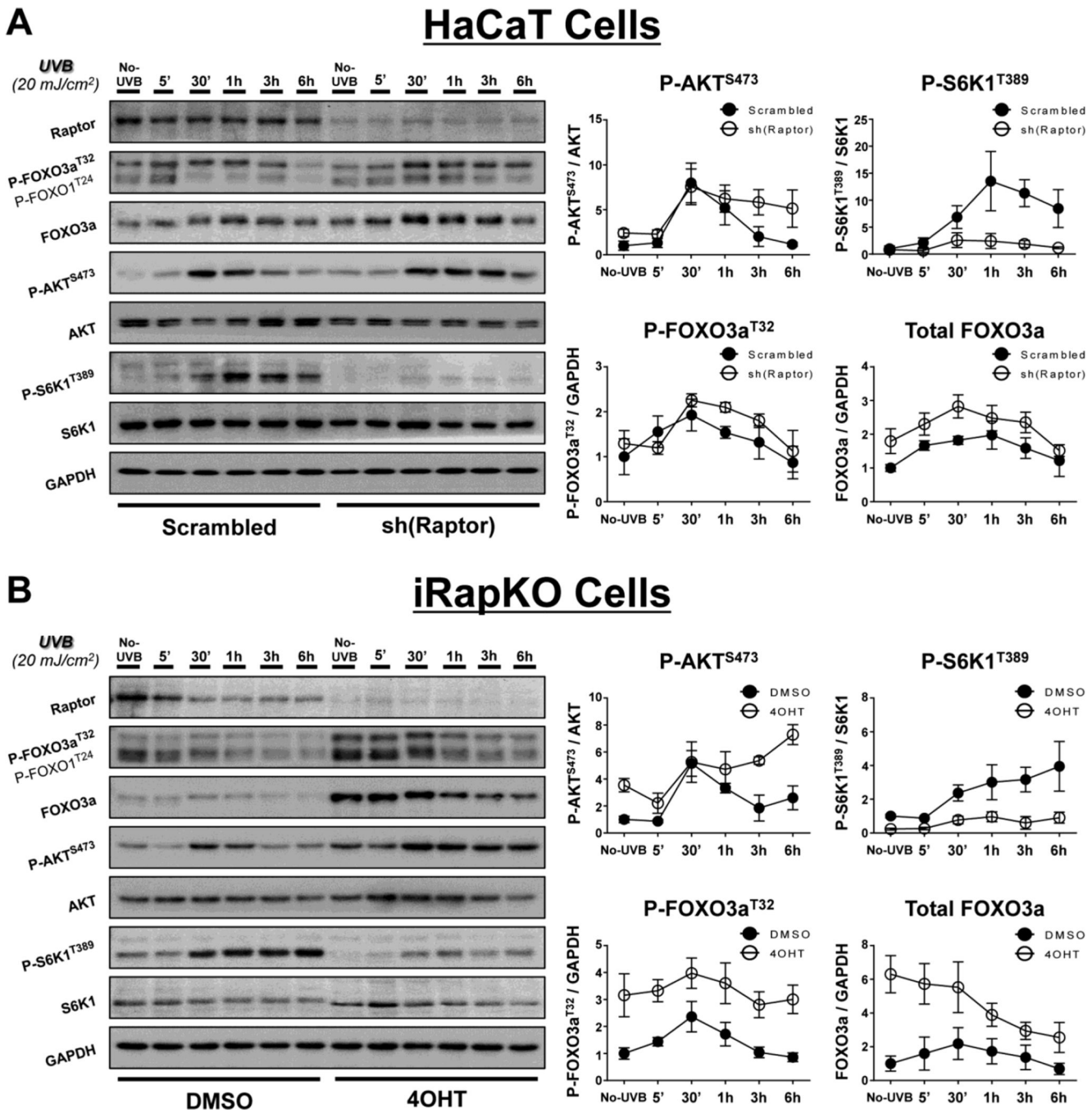

Fig. 2. Genetic disruption of mTORC1 increases both UVB-induced FOXO3a phosphorylation and FOXO3a protein levels

UVB exposure and immunoblot analysis were performed as described in Figure 1 for **(A)** HaCaT or **(B)** iRapKO cells with intact or disrupted mTORC1 signaling. mTORC1 was inhibited through **(A)** shRNA knockdown of Raptor in HaCaT cells [sh(Raptor)] or **(B)** 4OHT-induced recombination of a floxed *raptor* allele in iRapKO cells (4OHT), and compared to their respective controls (Scrambled or DMSO). The relative protein densities for both P-AKT^{S473} and P-S6K1^{T389} were normalized to their respective total protein while

both P-FOXO3a^{T32} and total FOXO3a were normalized to GAPDH. Quantitation of results is presented as the mean ± SEM of three independent experiments.

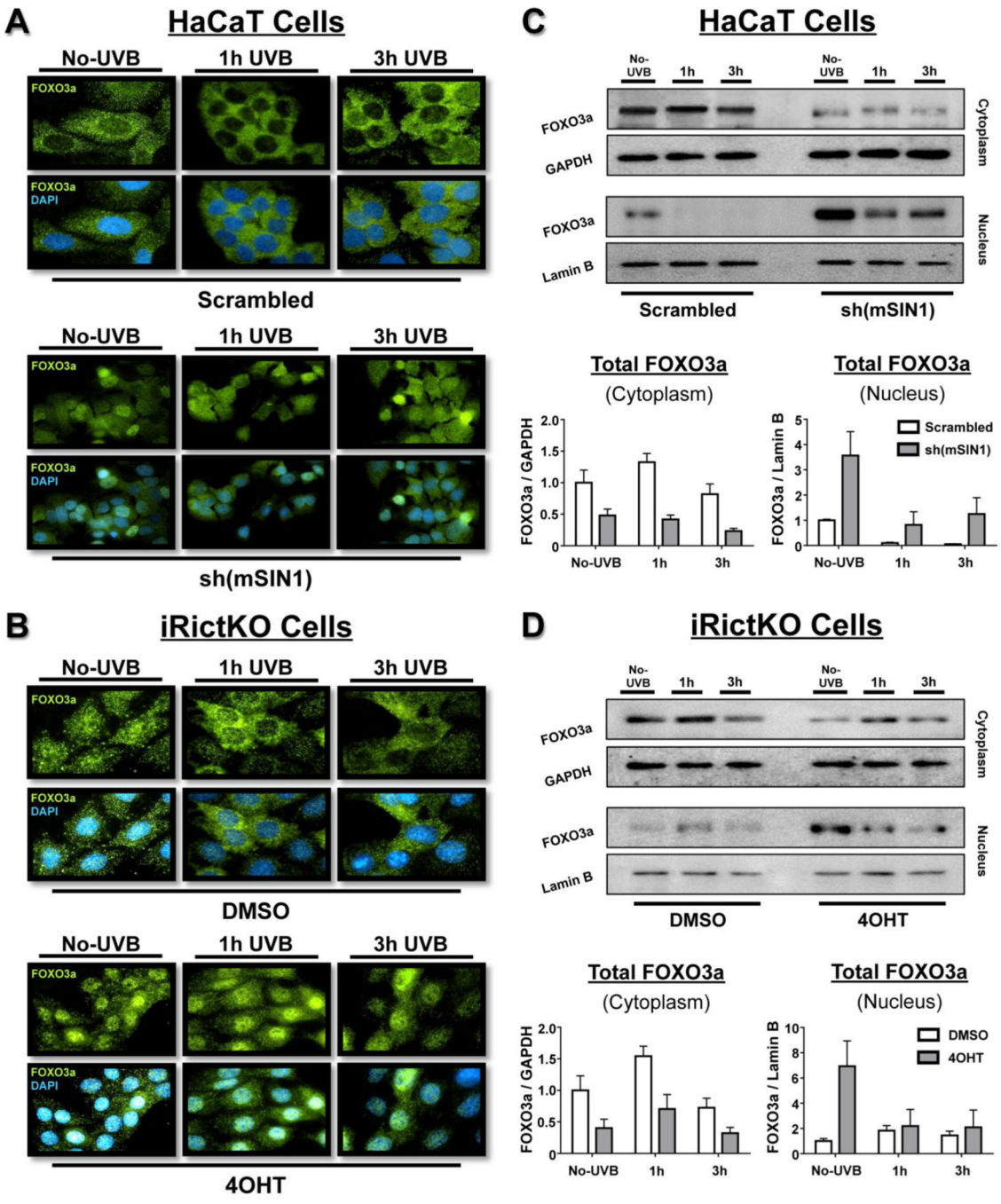

Fig. 3. Absence of mTORC2 activity increases relative nuclear FOXO3a localization and abundance both before and after UVB exposure

Time-course analysis of cells prior to (No-UVB) and up to 3 h following UVB (20mJ/cm^2) exposure. **(A, B)** Immunofluorescence (60× magnification) of FOXO3a (green) and DAPI (blue) of **(A)** HaCaT and **(B)** iRictKO with intact (Top Rows – Scrambled and DMSO respectively) or disrupted (Bottom Rows – sh(mSIN1) and 4OHT respectively) mTORC2 activity as described in the Materials and Methods. **(C, D)** Immunoblot analysis of both cytoplasmic and nuclear extracts of **(C)** HaCaT and **(D)** iRictKO cells in the presence or

absence of active mTORC2. Cells were exposed to UVB and both the nucleus and cytoplasm were isolated as described in the Materials and Methods. mTORC2 was inhibited using **(C)** shRNA knockdown of mSIN1 in HaCaT cells [sh(mSIN1)] or **(D)** 4OHT-induced recombination of a floxed *rictor* allele in iRictKO cells (4OHT), and compared to their respective controls (Scrambled or DMSO). The relative density for cytoplasmic FOXO3a was normalized to GAPDH while nuclear FOXO3a was normalized to Lamin B. Quantitation of results is presented as the mean ± SEM of three independent experiments.

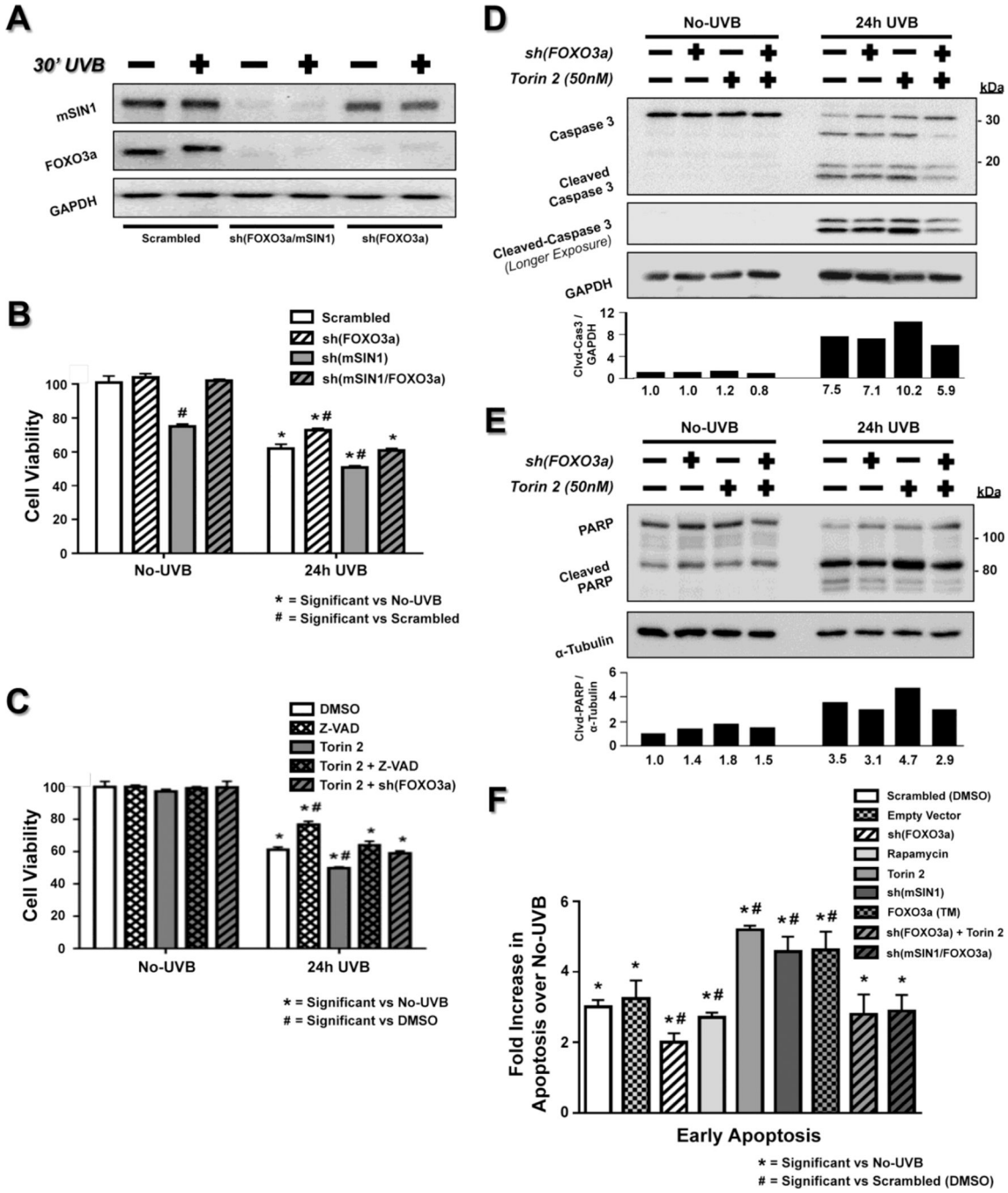

Fig. 4. Loss of mTORC2 sensitizes cells to UVB-induced apoptosis, which is rescued with knockdown of FOXO3a

HaCaT cells were exposed to UVB and analyzed for cell viability and apoptosis. **(A)** Immunoblot analysis of cells with knockdown of either FOXO3a [sh(FOXO3a)] or double knockdown of mSIN1 and FOXO3a [sh(mSIN1/FOXO3a)] before and 30 min post-UVB. **(B, C)** MTS cell viability assay for No-UVB control and 24 h after 35 mJ/cm^2 UVB irradiation in HaCaT cells treated with either **(B)** sh(mSIN1) or **(C)** 50 nM Torin 2 to block mTORC2 signaling, and in the presence or absence of sh(FOXO3a). Values are listed as %

cell viability and normalized to either **(B)** scrambled or **(C)** DMSO-treated HaCaT cells that were not exposed to UVB (n=12–18 biological replicates / group). The pan-caspase inhibitor Z-VAD FMK (50 μM) was used in **(C)** to examine the decrease in cell viability due to caspase-dependent apoptosis (Z-VAD, Torin 2 + Z-VAD). Immunoblot analysis (whole-cell extracts) of **(D)** Caspase 3 and **(E)** PARP following treatment of 50 nM Torin 2 in sh(FOXO3a) HaCaT cells 24 h after UVB irradiation (35 mJ/cm^2). The relative protein densities for cleaved caspase-3 were normalized to GAPDH and cleaved PARP values were normalized to α-tubulin. Quantitation of results is presented as the mean of two independent experiments. **(F)** Annexin V/7-AAD staining followed by FACS analysis was performed to measure early apoptosis 18 h post 35 mJ/cm^2 UVB for the indicated groups (n=3–6 biological replicates / group). A rapamycin treatment group was included to assess the effects of mTORC1 inhibition and transfection with the FOXO3a (TM) plasmid was used to mimic the regulatory effect on FOXO3a following mTORC2-disruption. Early apoptosis was expressed as percent of total cells that stained positive for Annexin V and negative for 7-AAD. For each treatment group, bars represent the fold change in early apoptosis versus their respective No-UVB control. Significance ($P < 0.05$) was calculated for both the MTS and FACS protocols as described in the Materials and Methods.

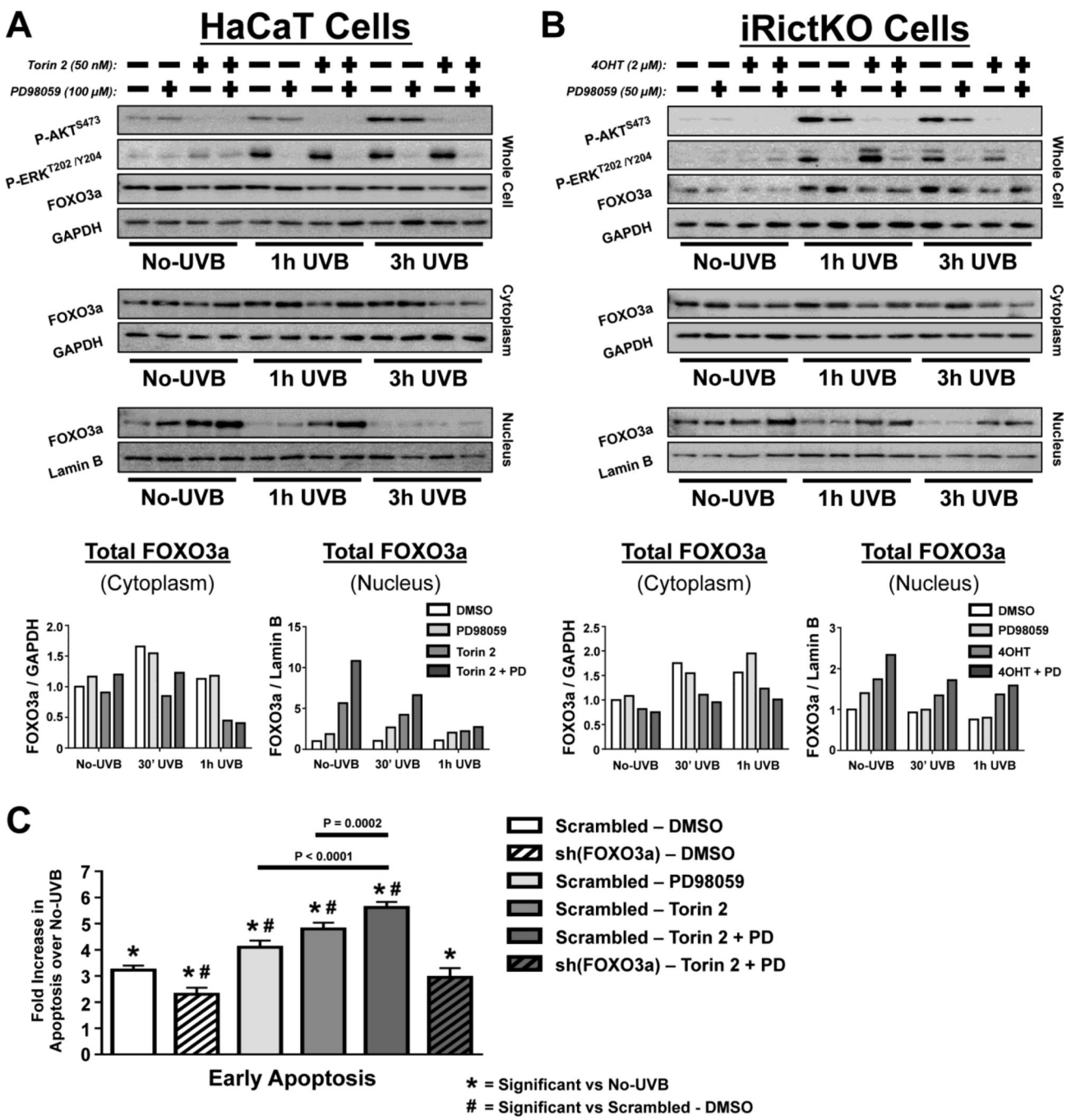

Fig. 5. Dual inhibition of mTORC2 and MEK signaling further increases relative FOXO3a nuclear abundance and apoptosis over inhibition of mTORC2 alone

Immunoblot analysis of mTORC2 & MEK signaling intermediates in No-UVB controls and up to 1 h after exposure to 20 mJ/cm^2 UVB. Whole cell, cytoplasmic, and nuclear extracts of **(A)** HaCaT and **(B)** iRictKO cells were harvested at the indicated times post-UVB and western blotting was performed with the antibodies indicated. mTORC2 signaling was inhibited by treatment with **(A)** 50 nM Torin 2 in HaCaT cells or by **(B)** 4OHT-induced recombination of a floxed *rictor* allele in iRictKO cells. MEK inhibition was accomplished

by overnight incubation using 100μM (HaCaT) or 50μM (iRictKO) PD98059 (PD). For dual mTORC2/MEK inhibition, Torin 2 + PD was used in HaCaT cells and 4OHT + PD in iRictKO cells. The relative density for cytoplasmic FOXO3a was normalized to GAPDH while nuclear FOXO3a was normalized to Lamin B. Quantitation of results is presented as the mean of two independent experiments. **(C)** Annexin V/7-AAD staining followed by FACS analysis was performed to measure early apoptosis 18 h post 35 mJ/cm^2 UVB for the indicated groups (n=3 biological replicates / group). Early apoptosis was expressed as percent of total cells that stained positive for Annexin V and negative for 7-AAD. For each treatment group, bars represent the fold change in early apoptosis versus their respective No-UVB control. Significance ($P < 0.05$) was calculated as described in the Materials and Methods.